RSC Advances

ROYAL SOCIETY OF CHEMISTRY

www.rsc.org/advances

Graphical Abstract:

GO was used as the wound dressing template. Normally GO can't be used directly in animal models due to its toxicity, hence it was functionalized with collagen and fibrin. Collagen was isolated from chrome shaving leather waste (CCLW) and fibrin was isolated from slaughter house blood waste, both the materials are obtained from environmental by-products.The prepared films were characterized, to establish the functionalization of GO. CFGO was used as a wound dressing material on the experimental wounds of rats and its efficacy was studied using biochemical, histological and general observations (schematic illustration)

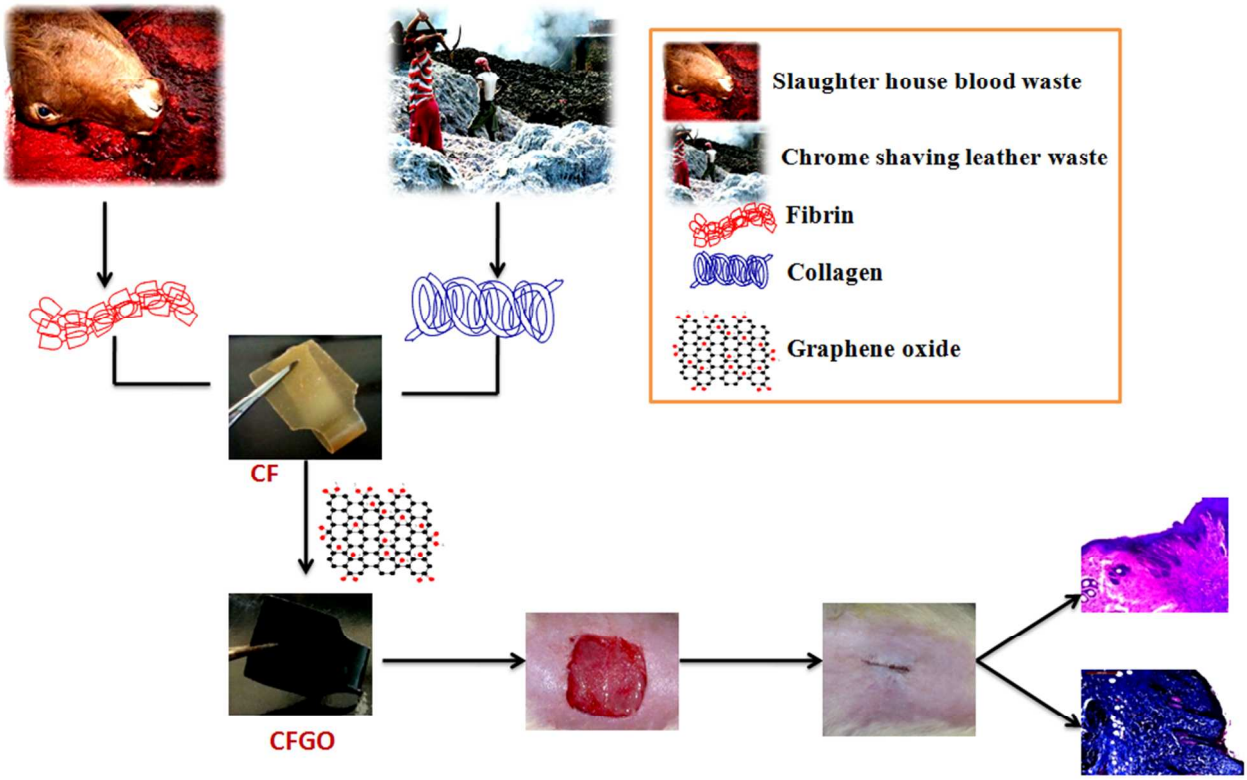

Graphene oxide incorporated collagen-fibrin bioflim as a wound dressing material

R. Deepachitraa, V. Ramnatha, T. P. Sastry[a*]

a Bio-Products Laboratory, Central Leather Research Institute, Adyar, Chennai 600020, India

***Corresponding author: Tel: 044 24911386, Fax: +91-44-24912150**

E.mail address: sastrytp@hotmail.com (T. P. Sastry).

Abstract

Functionalized graphene oxide offers many advantages as a biomaterial in various biomedical applications. In the present study graphene oxide (GO) was incorporated in the collagen-fibrin composite film (CFGO) and used as wound dressing material in both *in-vitro* and *in-vivo* studies. 3-(4, 5-dimethylthiazol-2-Y)-2, 5-diphenyltetrazolium bromide (MTT) assay using NIH 3T3 cells revealed that CFGO film is biocompatible. CFGO was also used as a wound dressing material on the experimental wounds of rats. Histopathalogical, biochemical and hematology studies have shown that the CFGO treated wounds healed faster than control and CF treated wounds. Based on the results CFGO can be used as wound dressing material in the smaller and larger animals.

Introduction

Graphene oxide (GO) is a single atomic plane of graphitecontaining abundant epoxide, hydroxyl and carboxyl functional groups on its basal plane and its edges provide many reactive sites for chemical functionalization and interaction[1,2]. Interactions between graphene and biological molecules are quite interesting in cell imaging, drug delivery, biosensors etc. Graphene nanosheets identically show some similar properties of carbon nanotubes (CNTs), but in the case of cytotoxicity studies single-wall and multi-wall CNTs show more toxicity to human and animal cells compared to graphene derivatives. This is due to the fact that GO is a two-dimensional structure and CNT's has only single dimension [3]. Due to concentration dependent toxicity, GO cannot be used directly in cell culture application, however, GO can be functionalized with biomacromolecules, for biomedical application. The potential of functionalized GO in cellular imaging, cancer therapy, drug delivery etc were reported by several authors [4-6]. These studies clearly indicate the bioactivities of surface modified GO.Graphene

derivatives functionalized with peptides, proteins, aptamers, avidin-biotin and other small biomolecules are used as building blocks for biodevices [5]. Multivalent functionalization and efficient loading of molecules on the substrate of GO suggests itsbiocompatibility in *in vitro* as well as in *in vivo* conditions [7-9]. Currently, few applications of GO derivatives are available in literature. Recently, it was proven that GO-based nano matrixes can act as promising system for the production of insulin [10]. A process for the multi-functional GO has been developed and was used as a fluorescence marker for *in vitro* and *in vivo* imaging [11]. GO was used as an efficient vascular endothelial growth factor (VEGF) delivery system in animal models, thereby suggesting its therapeutic application for treating ischemic disease [12]. Chitosan-Polyvinyl alcohol-graphene composites were prepared by electrospining method and studied for their antibacterial property and wound healing capacity and it was found that its antibacterial property helped in faster wound healing [13].

Chrome containing leather waste (CCLW) is the most prominent solid waste in tanning industry. CCLW is mainly used as a resource of collagen and chromium (III) complexes [14]. Using alkaline protease enzyme, under mild conditions protein products (gelatin and collagen hydrolyte) were isolated from chrome shavings which were potentially used in cosmetics, adhesive, printing, photography, micro encapsulation and as additives in leather industry [15]. Collagen is one of the structural proteins in the extracellular matrix of eukaryotes. It is the most abundant protein in vertebrates and constitutes about 30% of the total proteins present in skin, tendon, bone etc.Collagen molecules secreted by cells form characteristic fibers which are responsible for functional integrity of tissues such as bone cartilage, skin and tendon [16-18]. Collagen has a vital role in biomedical applications as wound dressing material, vitreous implant, drug carriers etc. Among various types, type I collagen is commonly found in mammalian

tissues. It shows good biocompatibility, biodegradability, weak antigenicity and superior surface-active properties when employed as a scaffold in tissue engineering [19-20].

Fibrinogen is converted as fibrin, which is a provisional matrix in wound healing process; its structural composition binds the cells and proteins and promotes cell adhesion, migration and proliferation [21-23]. It is a naturally occurring scaffold, which is used in angiogenesis, tissue repair and available in the form of sponge, film, powder, sheet etc. Fibrin glue helps in haemostasis and accelerates the wound healing. Fibrin sealant is used as improved wound healing material in diabetic patients. Bensaid et al [21] have reported that fibrin-based biomaterials are biocompatible, biodegradable and have high affinity to various biological surfaces. Sastry et al [24] have reported the preparation of physiologically clotted fibrin (PCF) from slaughterhouse wastes that could be used for biomedical purposes such as wound healing and osteoinduction.

Research on wound healing agents is one of the developing areas in modern biomedical sciences. Wound healing involves continuous cell–cell and cell– matrix interactions in response to an injury that restores the function and integrity of damaged tissues. There are many commercially available wound dressing materials in market based on gelatin, carboxymethylcellulose, collagen, pectin etc [25, 26]. These materials are used individually as well as in various composite form. The aim of the present work is to prepare a wound dressing material in the form of composite filmcontaining collagen and fibrinimpregnated with GO.

Results and Discussion

Normally, GO can't be used directly in animal models due to its toxicity, hence it was functionalized with collagen and fibrin (CFGO). The prepared films were characterized, to establish the functionalization of GO. CFGO was used as a wound dressing material on the experimental wounds of rats and its efficacy was studied using biochemical, histological and general observations (Fig. 1 schematic illustration)

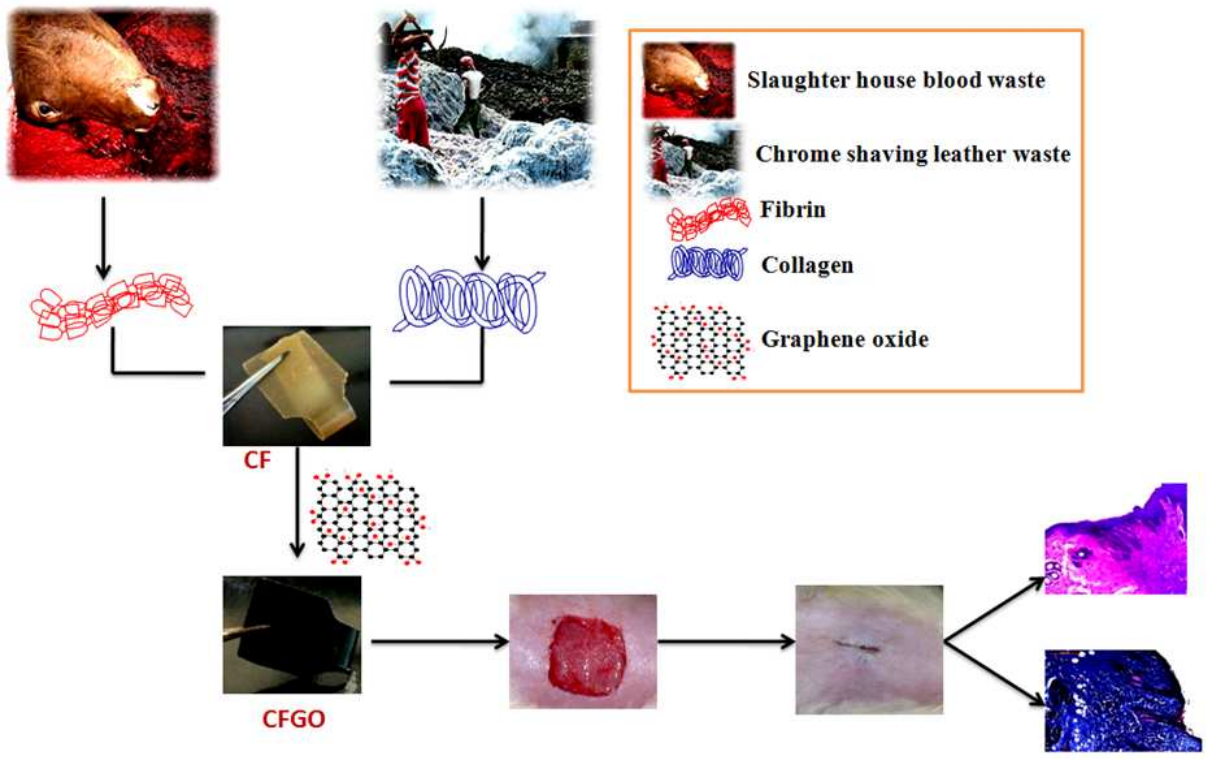

Fig. 1 Schematic illustration of CFGO as wound dressing material.

The mechanical properties of a wound dressing material play a vital role when it is used in *in vivo* applications. The mechanical properties of composites are given in table 1, 2 and 3. When compared to collagen, fibrin alone has lesser tensile strength, whereas the combination of both shows improved mechanical strength. Among the different stoichiometric ratios used , CF film

which exhibited better tensile strength was selected and was further used to prepare CFGO films with different stoichiometric ratios of GO (Table 3); 0.01% of GO has shown approximately two fold higher tensile strength. Hence, this composite film was used in further experiments. Ethylene glycol was used to improve the flexibility of the films [27,28].

Table 1

Sample no	F:C (%composite)	Elongation at break (%)	Tensile strength (MPa)
1	1: 0	0.78±0.87	16.43±4.67
2	1: 0.2	3.23±0.94	18.04±5.27
3	1: 0.4	7.18±1.56	27.53±4.37
4	1: 0.6	7.77±1.45	29.22±3.54
5	1: 0.8	3.59±2.67	20.16±5.16
6	1: 1	3.24±1.42	18.54±3.24

Table 2

Sample no	C:F (%composite)	Elongation at break (%)	Tensile strength (MPa)
1	1: 0	1.78±0.34	24.43±3.67
2	1: 0.2	3.23±1.45	29.5±3.56
3	1: 0.4	4.57±1.67	37.36±4.23
4	1: 0.6	6.62±2.45	45.5±4.67
5	1: 0.8	10.8±3.81	48.55±5.87
6	1: 1	8.41±2.1	41.41±3.52

Table 3

Sample no	C:F:GO (%composite)	Elongation at break (%)	Tensile strength (MPa)
1	1: 0.8: 0.001	6.4±0.67	40.43±3.56
2	1: 0.8: 0.003	14.8±1.34	47.36±4.45
3	1: 0.8: 0.005	11.8±2.35	57.5±5.34
4	1: 0.8: 0.01	9.62±1.25	78.55±5.74
5	1: 0.8: 0.02	9.43±2.45	71.41±3.67

Tables 1, 2 and 3- Physiochemical properties of various stoichiometric ratios of collagen, fibrin and graphene oxide composites.

Infra-red spectra (Fig. 2a) of C, F and CF composites showthe amide I peaks at 1637, 1644 and 1634 cm^{-1}, amide II peaks at 1549, 1539 and 1541 cm^{-1}, amide III peaks at 1241, 1238 and 1243 cm^{-1} respectively; peaks at 1453, 1451 and 1453 cm^{-1}correspond to $–CH_2$ moiety of C, F and CFrespectively [29]. IR spectrum of GO shows the presence of υ (C-O) of –COOH groups at 1734 and 1626 cm^{-1}, carboxyl group at 1401 and alkoxy group at 1058 cm^{-1}[10]. CFGO composite shows the absence of a peak at 1734 cm^{-1} which represents the reduction of carboxyl moiety on the surface of GO with the addition of C and F. CFGO represents amide I, II and III peaks at 1634, 1541 and 1242 cm^{-1} respectively. XRD spectra (Fig. 2b) of GO shows a peak at 11.2° which represents the presence of more oxygen functional groups on the basal plane of graphene sheet. This sharp narrow peak intensity is lesser withthe addition of C and F in CFGO; in addition the presence of peak at 20.6° indicates the presence of protein addition, in CF this peak is present at 20.4°. This shows that the addition of GO does not alter the structure of CF.

Raman spectrum of GO shows the presence of D band at 1366 cm^{-1} which represents the vibrations of sp^3 carbon atoms and the band at 1601 cm^{-1} represents sp^2 hybridized carbon atom of GO (Fig. 2c) [30]. CFGO represents amide II and III peaks at 1543 and 1242 cm^{-1}, however, amide I peak is absent, in addition lesser intensity peaks of D band at 1347 and G band at 1598 cm^{-1} were observed (Fig. 2c) when compared to those of GO, this may be due to the interaction between the GO and CF.

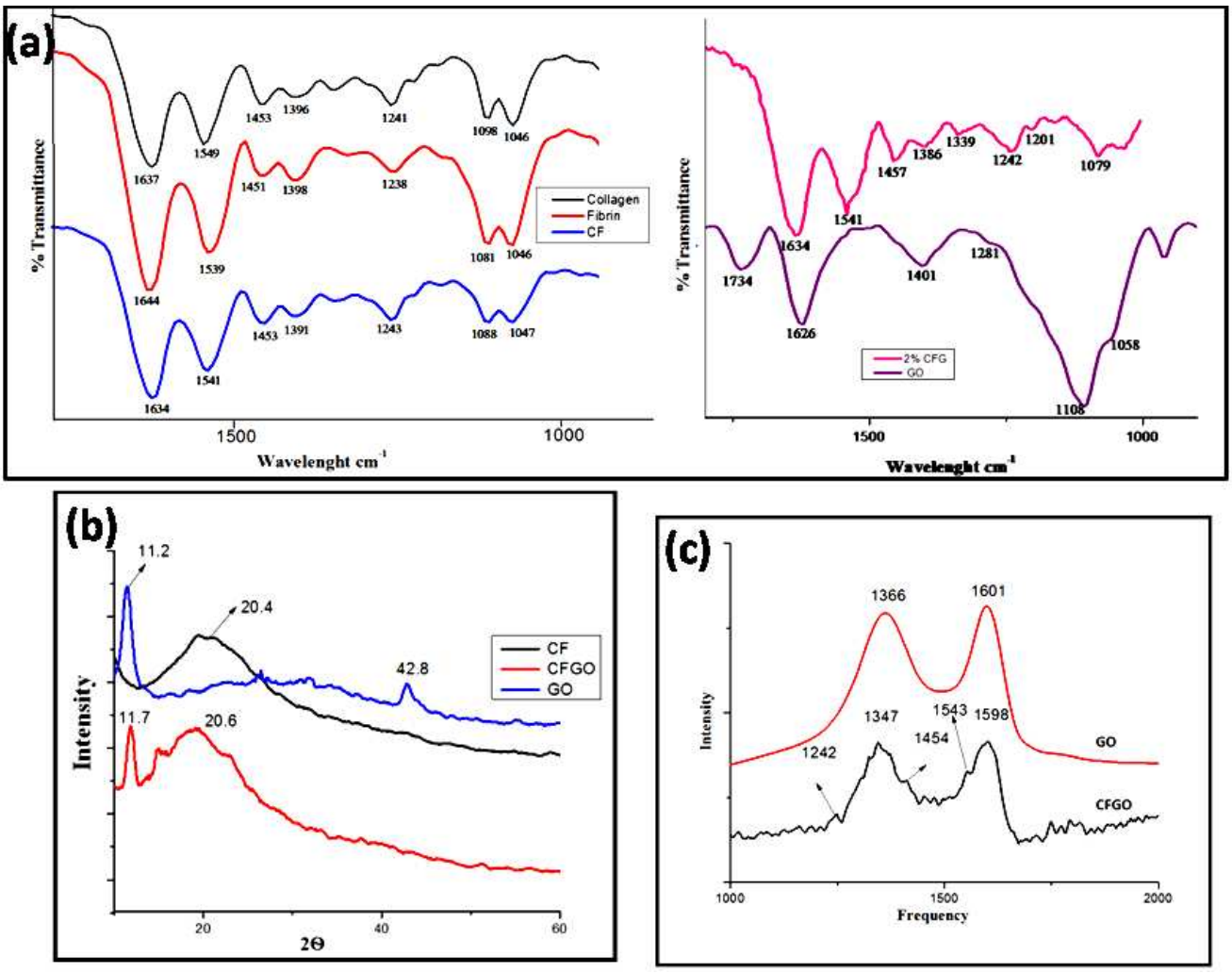

Fig. 2- (a) FTIR spectra of collagen, fibrin, CF, GO and CFGO. (b) XRD spectra of GO, CF and CFGO. (c) Raman spectra of GO and CFGO

Scanning electron microscopy (SEM) images of GO, CF and CFGO are shown in (Fig. 3a). GO shows agglomeration of ultrathin sheets; the surfaceof CF was smooth and porous in nature. Presence of GO was evident in CFGO and it had retained its porosity even after the addition of GO. AFM images (Fig. 3b) of GO, CF and CFGO also indicate the smooth surface of the films and have similar morphology compared to those of SEM. The porous nature of the films helps in absorbing wound fluids and keeps the wound surface dry, and it will also help in oxygen supply to the wound [29].Water absorption capacity (Fig. 3c) is an important property to keep the

wound surface dry and for enhancing wound healing. Water absorption capacity of CF and CFGO showthat CFGO has high water absorption values when compared to CF and this may be attributed to the presence of more hydrophilic groups like –OH, $–NH_2$, etc., on its surface. Already GO contains functional groups like –COOH, –C=O, –OH, and –C–O–C– on its surface. Functionalization with collagen and fibrin has further increased the hydrophilic groups of the protein networks [31].The degradation rate of CFGO (Fig. 3d) is higher when compared to CF, this may be due to its more hydrophilic nature.

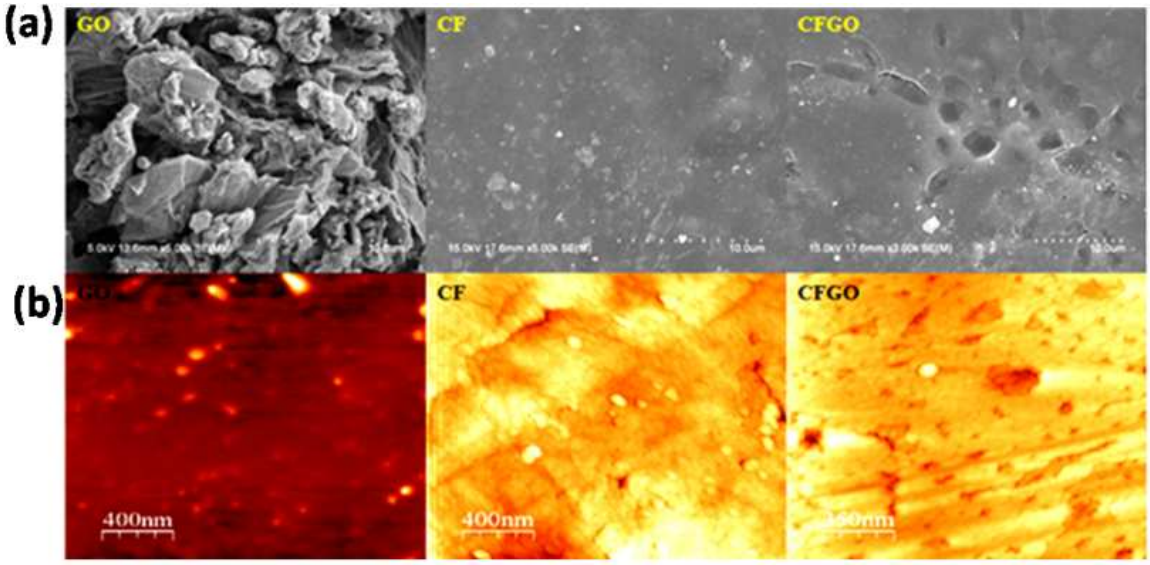

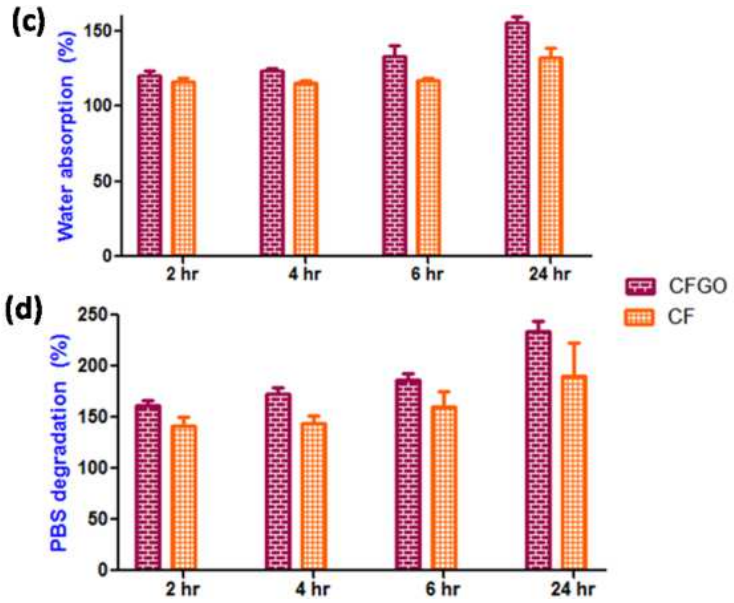

Fig. 3- (a) SEM images of GO, CF and CFGO. (b) AFM images of GO, CF and CFGO. (c) Water absorption studies of CF and CFGO composite films. (d) Degradation rates of CF and CFGO composite films using PBS buffer.

MTT assay was carried out using normal fibroblast (NIH 3T3) cells. Cells treated with GO, CF and CFGO were incubated for 1, 4 and 7days. The results revealed that (Fig. 4a) CF exhibited 100% cell viability till 7 days, and have shown higher cell proliferation rate compared to control. GO treated cells showed significant ($p \leq 0.05$) decrease in cell viability, whereas addition of GO with CF has improved the cell viability percentage. There was no significant difference between the control and CFGO treated groups, throughout the study. According to previous studies, GO enhances more cell adherence and proliferation than pristine graphene due to abundant oxide groups on its surface. At low concentrations, GO induces stronger metabolic cell activity, and this is reversed at high concentrations. GO produces cytotoxicity in concentration and time dependent manners and can enter into the cytoplasm (lysosome, mitochondrion, and endoplasm) and nucleus, which decreases cell adhesion and induces cell floating and apoptosis [32]. But in

thecase of CFGO reduced toxicity was observed, this isbecause of functionalization of GO by CF, Fig. 4b shows the inverted microscopic images of the cell viability on day 1 of all treatments and control.

Hemolysis assay revealed the effect of GO, CF and CFGO against blood components (Fig. 4c). GO revealed significant hemolytic property compared to the control, which could be due the presence of abundant negatively charged carboxyl groups that are highly concentrated at the edges of GO; there may be strong interactions (electrostatic and hydrophobic interactions) between the amphiphilic GO and the lipid bilayer of the blood cell membrane [5]. The chemical structure of GO endows it with surfactant-like performance, which has adsorption ability at the interfaces and could lower the surface or interfacial tension [33] thus, small sized GO may act as a molecular surfactant and large sized GO can behave like a molecule–colloid dualistic surfactant. Thus, when GO is exposed to blood cells, it may lead to severe hemolysis [34,35]. However, the effect was less when compared with the positive control (Triton X 100). Interestingly, hemolytic properties were much reduced in CFGO when compared to GO which could be attributed to the functionalization of GO with CF. CFGO might have difficulty in interacting with the lipid bilayers, [34] thereby suppressing the hemolysis.

Reactive oxygen site (ROS) is a common toxicity mechanism of carbon-based and other nanoscale materials; ROS initiates the dysfunction of mitochondria and induces the cell cytotoxicity. According to clinical studies, materials with small size and large surface area enhance the ROS [36-38]. In the present study, GO has induced ROS in the cells, results are shown in Fig. 4d. GO induces cytotoxicity by causing physical damage to the cell membrane which results from direct interactions between the cell membrane and GO nanosheets. Electrostatic interactions occur between negatively charged oxygen functional groups in GO and

positively charged Phosphatidylcholine lipid of cell membranes [39]. Significant reduction ($p \leq 0.05$) in ROS levels was observed in CF and CFGO treated cells compared to GO treatment. Fluorescence microscopic images of treated cells are shown in Fig. 4e. 2′,7′ dichlorofluorescindiacetate (DCFH) reacts with ROS to form DCF, the fluorescent product. More numberof ROS induced fluorescence cells were appeared at positive control lipopolysaccaride (LPS), however, CF and CFGO did not show much ROS induced cells.

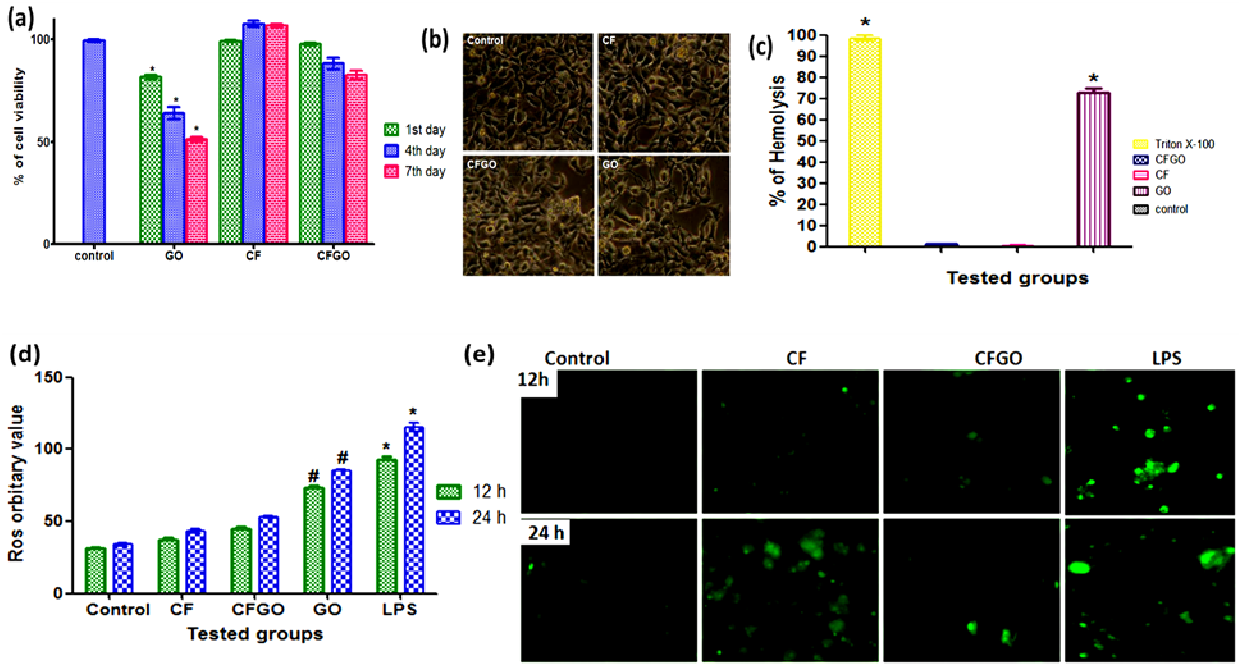

Fig. 4 – (a) MTT Assay representation of GO, CF and CFGO. (b) The microscopic images show the cell viability of those treatments on 1st day. Significance difference ($p \leq 0.05$) occurred between GO and control. (c) Hemolytic assay representation of GO, CF, CFGO and Triton X-100. Significant difference ($p \leq 0.05$) occurred between triton X-100 and GO. (d) ROS generation of GO, CF, CFGO and LPS treated cells and (e) fluorescence microscopic images of treated cells. Significance difference ($p \leq 0.05$) occurred between control and other treatments.

Surface of the wounds were photographed periodically from a constant distance for both control and experimental animals (Fig. 5a). Faster rate of healing was observed in the experimental wounds compared to those of control. The results are in agreement with those of planimetric observations. On the 4th day, the wound contraction of control was 28% whereas 33% and 42% closure were observed in CF and CFGO treated wounds respectively. However, by the 12th day, 82% of the wound was closed in the CF experimental groups; 97% of the wound was closed in the CFGO experimental groups, whereas 72% closure was observed in control. These results show the efficacy of CF and CFGO as wound dressing materials. The presence of GO in CF films accelerated wound healing on 12th day itself , according Lu et.al 2012, graphene accelerated wound healing in experimental animals due to its antibacterial activity [13]. According to our results the presence of GO exhibited better wound healing property compared to CF and control.The following mechanism might have enhanced the wound healing process: The presence of collagen and fibrin in CFGO would have caused moderate ROS generation in wound healing process [40]. Graphene impede the prokaryotic cells and not the eukaryotic cells, this antibacterial efficiency enhances faster wound healing. This may occur due to the electron transfer from graphene into the nucleus of prokaryotic cells which are devoid of nuclear membrane [13]. Further, due to better water absorption property of CFGO, the surface of the wound is dry and this might have avoided the bacterial infection on wound surface [29, 41, 42].The higher rate of 3T3 fibroblast cell proliferation in CFGO treated cells in*in-vitro*is an indication for the faster wound healing mechanism in *in-vivo*.

Histological studies of treated and control groups were studied by using H&E and Masson trichrome staining (Fig. 5b&c). On 4th day CFGO and CF treated groupshave shown acute and chronic inflammatory cells such as neutrophils and lymphocytes with blood vessels

and extravessated RBC's. Inflammatory cells promote the migration and proliferation of endotheial cells, which leads to neovascularisation. This in turn aids in repithelialization of the wounded tissue [43]. On 8th day when compared to control, treated grouphas shown moderate inflammatory cells. Fibrous nature of connective tissues with less inflammatory cells and red blood vessels were clearly monitored in CFGO treated groups which facilitated the faster wound healing. On 12thday CFGO treated groups have shown epithelium and connective tissue formation; the density of collagen fibers is high in CFGO, compared to those of CF and control. On 12th day CF treated groups have shown moderate epithelialization. The collagen deposition and faster epithelial formation in CFGO could have significantly accelerated better wound healing compared to other treatments. Masson's trichrome staining helped to clearly visualize the changes in collagen fibers. On 8th day, formation of new collagen fibers was more prominent in CFGO treated groups compared to CF and control. Proliferation of fibroblasts, which are the major producer of collagen, was also observed. Masson's trichorme staining clearly shows the blue colour of collagen fibers. Collagen remodeling and degradation occurs simultaneously to provide the tensile strength and reduce scar formation [44]. Other than collagen, MT staining also helps histopathologists differentiate other anatomical structures and organelles in the healed skin such as scab, fine and coarse collagen fibers, hair follicle and adipose tissue [45].Faster wound healing and deposition of collagen did not contribute any scar formation in the wounded area. This indicates CFGO might be used as a wound dressing material which effects a scar less healing.

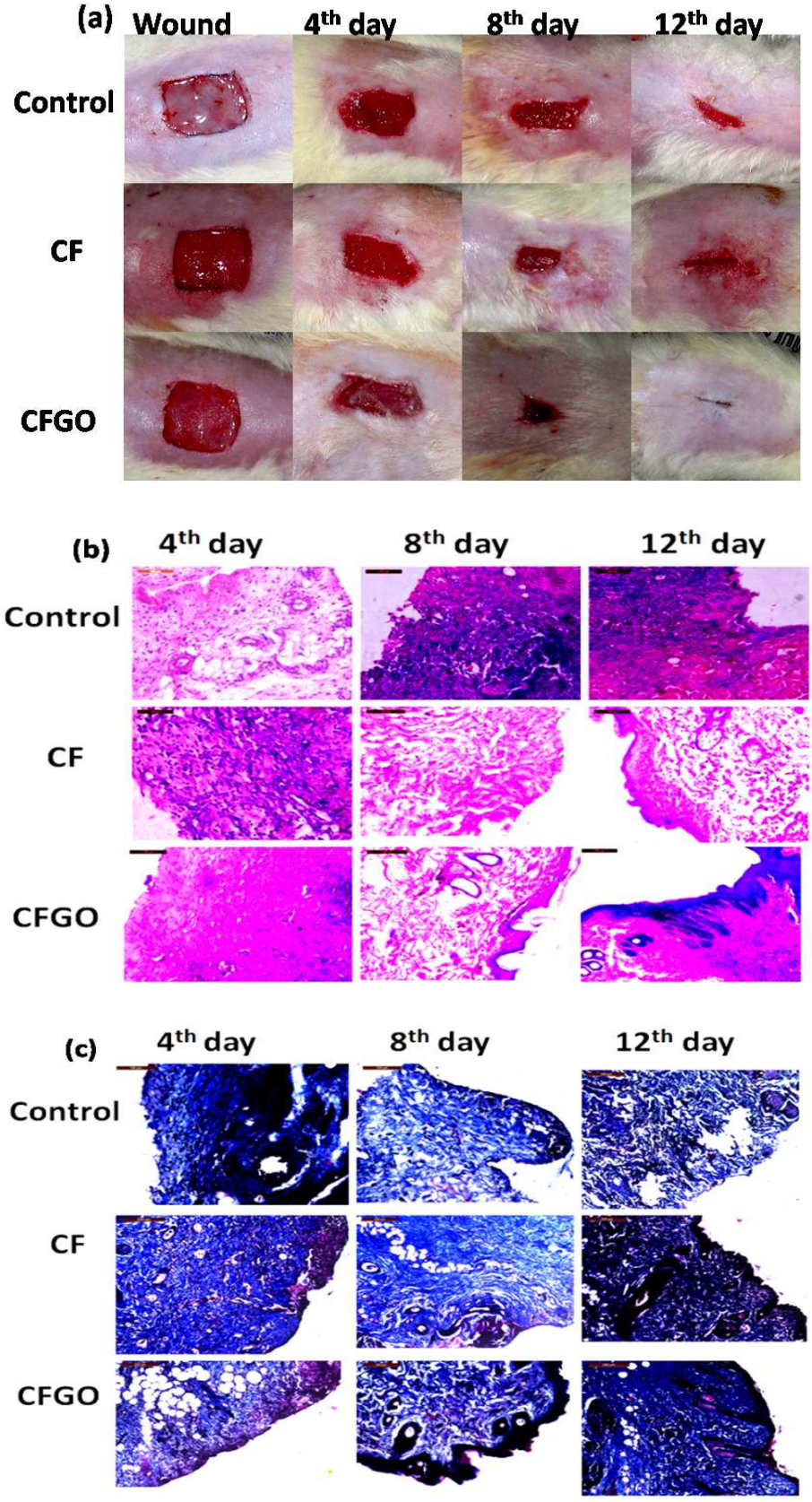

Fig. 5 (a) Photographic evaluation of wound healing. Faster healing was observed on 12th day in the CFGO treated rats. (b) Histological section of H&E staining on control, CF and CFGO treated woundsupto 12 days post wound. (c) Histological section of Masson trichorme staining on control, CF and CFGO treated wounds upto 12 days post wound.

The biochemical parameters i.e., collagen (Fig. 6a), hexosamine (Fig. 6b) and uronic acid (Fig. 6c) were analyzed in the granulation tissues of experimental rats on different days after wound creation. The concentration of collagen in CFGO treated wounds increased till 8th day and later decreased on 12th day. This noticeable increase might be due to increased synthesis of collagen and could be correlated to the effective healing of wounds. Since collagen is the predominant extracellular protein in the granulation tissue of a healing wound, rapid increase in the synthesis of this protein indicated faster wound healing. Hexosamine, a matrix molecule, act as ground substratum for the synthesis of new extracellular matrix. The glycosaminoglycans are known to stabilize the collagen fibres by enhancing electrostatic and ionic interactions and possibly control their ultimate alignment. Their ability to bind and alter protein-protein interactions has identified them as important determinants of cellular responsiveness in development, homeostasis, and disease [46]. In our study, prominent increase in the levels of hexosamine in treated groups was observed compared to that of control group. Similar trend was observed inthe contents of uronic acid. Increase in the levels of collagen, uronic acid, and hexosamine in the treated groups gave an indication of the faster rate of wound healing compared to controls [26].

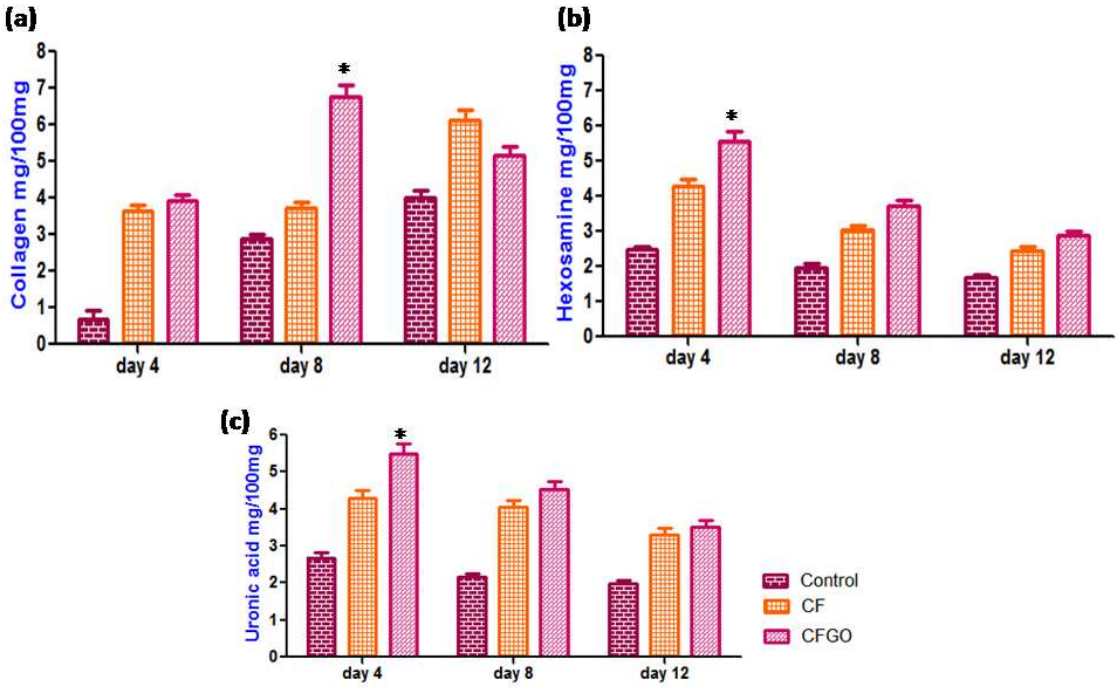

Fig.6 (a) Collagen content, (b) Hexosamine values and (c) uronic acid values of granulation tissue in control, and experimental wounds. Collagen content of CFGO treated rat's increased upto 8th day and later decreased. Hexosamine and uronic acid value shows the decreasing trend in both control and treated rats. Significant difference ($p \leq 0.05$) occurred between control and CFGO treated tissues.

Tensile strengthvaluesof healed wounds of treated groups were higher when compared to those of control group (Table 4). Increased tensile strength indicates maturation of collagen by formation of inter-and intramolecularcrosslinking. In case of control wounds, the decreased tensile strength may be due to the delay in the maturation of collagen. CFGO might have enhanced the epithelization process and hastened the deposition of collagen which has resulted in the better tensile strength in the experimental wounds. Normally, tensile strength is directly related to the amount of collagen synthesized at the wound site [47]. The hematological parameters were studied on 12th day on both treated and control rats (Table 5). There was a

significant ($p \leq 0.05$) increase in the values of hemoglobin, platelets, lymphocytes etc in CFGO treated groups compared to those of control. The results revealed that the films caused no adverse effects under *in vivo* conditions, which were in agreement with the *in vitro* biocompatibility studies [48].

Table 4

Group	Elongation at break (%)	Tensile strength (MPa)
Control	5.67±3.67	0.35±0.89
CF	9.90±5.78	0.94±0.67
CFGO	**42.50±7.89**	**1.63±0.98**

Table 4 -Tensile strengths of healed skins of rats of control and experimental groups

Table 5

	Control	CF	CFGO
WBC (10^9/µL)	8.85±2.3	5.2±0.4	3.6±1.3
RBC (10^{12}/µL)	4.09±2.6	8.65±0.6	10.09±2.7
Hb (g/dL)	11.6±1.3	13.78±1.2	15.4±1.4
HCT (%)	27.3±2.4	50.7±1.2	40.8±2.1
MCV (fL)	66±1.7	53±0.6	58±2.1
MCH(pg)	28±2.3	17.8±0.3	15.8±0.6
MCHC (%)	42±2.4	33±0.5	30±0.9
Platelet (10^3/µL)	665±1.4	553±0.7	498±3.6
Lym (%)	43.7±1.6	60.5±0.8	78.65±1.2

Table 5 - Comparison of hematological values between treated and control groups of rats after 20 days post wounding.

Conclusion

Collagen-fibrin biocomposite films incorporated with GO were prepared. Presence of GO increased the mechanical strength of collagen/fibrin composite films.*In-vitro* studies revealed the biocompatible nature of CFGO. Faster wound healing was observed in CFGO treated rats compared to those of CF and control. The present study indicates that functionalized GO enhances wound healing and CFGO may be tried on more clinical wounds of smaller and larger animals before its application on to humans.

Acknowledgments

R. Deepachitra gratefully acknowledges the financial support provided by Department of Science and Technology (DST).

Experimental section

CCLW was obtained from local leather tanning industry, crude fibrin was collected from nearby Municipal slaughter house and other chemicals used in this study were analytical reagents and purchased form Sigma Aldrich Co. India.

CFGO Bio film synthesis

Graphene oxide was prepared according to modified Hummers method [49]. The obtained GO was further dialyzed for 24 h using water and then it was dried at 60°C. The powdered GO was further sonicated to get a well dispersed solution with different ratios (0.001%, 0.003%, 0.005%, 0.01% and 0.02%).

Collagen was isolated from chrome containing leather waste as described earlier [47]. The collagen was further purified by dialyzing against 0.1M acetic acid and distilled water respectively for 24h. The sample was freeze-dried and used as such. Physiologically clotted crude fibrin was separated from fresh blood by churning as described earlier [23]. Fibrin was

further purified by wet precipitation method, 1g of final content was dissolved in 10 ml of 1N NaOH solution; the pH was adjusted to 5 to get white precipitation of purified fibrin. This was dialyzed against water for 24h to get purified fibrin. The sample was freeze-dried and used as such.

Collagen-Fibrin (CF) films were prepared by the mixing different stoichiometric ratios of fibrin and collagen as described in Table 1&2. From Table 2, the CF composite which exhibited better tensile strength was selected and further mixed with different stoichiometric ratios of GO to prepare CFGO films described in Table 3. From Table 2&3, the better composites which exhibited better tensile strength was selected and used for further experiments. Ethylene glycol was added as plasticizing agent. This mixture was poured into polythene trays (measurement 12 cm x 7.5 cm) and dried at room temperature (30˚C) to get CFGO in sheet form.

Characterization

Tensile strength properties were measured using three dumb-bell shaped specimens of 4 mm wide and 10 mm length of prepared films. Mechanical properties such as tensile strength (MPa) and percentage of elongation at break (%) were measured using a Universal testing machine (INSTRON model 1405) at an extension rate of 5 mm/min.

Fourier transform infrared (FTIR) measurements were carried out to determine the formation and changes in the functional groups on the prepared composite films. The spectra were measured at a resolution of 4 cm^{-1} in the frequency range of 4000–500 cm^{-1} using Nicolet 360 FTIR spectrometer. The X-ray powder Diffraction (XRD) patterns were done withSeifert JSO Debyeflex 2002. X-ray Diffractometer (30 mA,40 kV) using Cu Ka radiation (k = 0.154056 nm). The FT-Raman spectrum was carried out using Bruker Rfs 27 FT-Raman spectrometer, with a scanning range of 50-4000cm^{-1}.

Surface morphology of the samples was visualized by scanning electron microscope (SEM Model LEICA stereo scan 440). The samples were coated with gold ions using an ion coater (Fisons sputter coater) with following parameters: 1 Torr pressure, 20 mA current, and 70s coating time, using a 15 kV as accelerating voltage. Atomic force microscopy (AFM) was done with Agilent Pico LE Scanning Probe Microscope model. The Agilent instrument is a tip scan instrument, equipped with small (10 ml) and large AFM scanners (150 ml). This instrument is equipped with an environmental chamber, capable of heating to 200°C.

The water absorption capacities of CF and CFGO biocomposites were determined according to the method followed by Sastry and Rao [50]. To measure the degradation rate, the weight of the scaffold was measured as a function ofdegradation time. Three specimen of all scaffolds were equally weighed (W_0) and then immersedin phosphate buffer solution (PBS) (pH 7.4) for 24 h. The temperature wasmaintained at 37˚C. After predetermined periods of soaking time, each specimen was taken outand kept for 24 h. These were then weighed (W_T). The percentage of weight loss was given by the following equation,

$$\text{Weight loss (\%)} = [(W_0-W_T)/W_0]*100$$

***In vitro* studies**

NIH-3T3 cells were grown in a 96-well plate. The cell viability was measured after 1st day, 4th day and 7th day using 3-(4, 5-dimethylthiazol-2-Y)-2, 5-diphenyltetrazolium bromide (MTT) and 10% dimethyl sulfoxide (DMSO). The assay was performed in triplicates and the untreated wells were maintained as control [51].

Haemolytic assay was carried out to evaluate the safety of films for *in vivo* application [52]. Blood was collected from healthy rats [Ethical Approval: IAEC No. 11/2014 (a)] in a heparin sodium-containing tube and centrifuged at 10,000 ×g for 10 min. Pellet containing RBCs

was diluted in 20 mM HEPES buffered saline (pH 7.4) to 5% v/v solution. RBC suspension was treated with CF and CFGO and incubated at 37°C for 60 min. RBCs treated with 1% Triton X-100 served as positive control [53]. After incubation, all the samples were centrifuged and the supernatants were used for measuring optical density at 540 nm.

The oxidant-sensitive dye 2',7'-dichlorfluorescein-diacetate (DCFH-DA) was used for ROS detection. Lipopolysachharides (LPS) treated macrophage cells were treated with CF and CFGO films for 12 and 24 h. The effect of films on ROS was studied with the help of DCFH-DA, which enters cells passively and is deacetylated by esterase to non-fluorescent DCFH. DCFH reacts with ROS to form DCF, the fluorescent product. Fluorescence was read at wavelengths of 485 nm for excitation and 530 nm for emission with a fluorescence plate reader (TECAN). Untreated wells served as control and LPS (alone) treated wells served as positive control. [54]

2.4 *In vivo* studies

In vivo experiments were preformed according the Institutional Animal Ethical Committee approval and guidelines: IAEC No. 11/2014 (a). 30 Male albino Wistar rats (150-200 g weight) were chosen and they were divided into three groups (n=3). Throughout the experiment, rats were maintained in an air-conditioned room at 25±1°C with a proper lighting schedule of 12 h light and 12 h dark cycle. The animals received commercial rat diet and water *ad libitum*.

Each animal was given a dose of sodium pentobarbital (40 mg/Kg body weight) intraperitonally. The dorsal surface of the rat below the cervical region was epilated under aseptic conditions. An open excision wound of 2 cm × 2 cm was created on the shaved dorsal side of rats using sterile surgical blade. Control group wounds were dressed with, sterile cotton gauze dipped with gentamicin, while wound dressing films of CF and CFGO were applied separately on

experimental wounds. The dressings were periodically changed at an interval of 4 days with the respective materials. Three rats were sacrificed periodically on 4^{th}, $8^{th}$and 12^{th} day of post wound creation and the granulation tissues formed were removed and stored at −70°C until analysis. The progress of wound healing in the three groups was evaluated visually, planimetrically, histologically and biomechanically by periodical monitoring of wound surface.

Hair was clipped around the scar for proper visualization and the individual contour of the wounds of both control and experimental animals was measured periodically, using a transparent graph sheet and the rate of healing was calculated and expressed as percentage contraction.

In the present study, collagen, hexosamine and uronic acid levels were estimated in the granulation tissue of control and experimental wounds on 4^{th}, $8^{th}$and 12^{th} days. The granulation tissue was collected after sacrificing the animals on the respective days. Collagen and hexosamine were determined in defatted dried granulation tissue by the methods of Woessner [55], Elson [56] and Morgan [57] respectively. Extraction of uronic acid from the tissue was carried out according to the method of Schiller [58] and estimated by the method of Bitter and Muir [59].

The animals were sacrificed periodically on 4^{th}, 8^{th}, and 12^{th}days post wound creation and the tissue from the wound site of the individual animal was removed. These samples were then separately fixed in 10% formalin, dehydrated through graded alcohol series, cleared in xylene, and embedded in paraffin wax (m.p. 56°C). Serial sections of 5 μm thickness were cut and stained with hematoxylin and eosin and Masson's trichrome. The sections were examined under a microscope and photomicrographs were taken.

Blood was collected from rats when they were sacrificed at 12^{th} day, during the wound healing process. Hematological parameters such as hemoglobin ,total WBC Count, differential leucocyte

count, erythrocyte sedimentation rate, total RBC count, platelets, packed cell volume, mean corpuscular volume, mean corpuscular hemoglobin, mean corpuscular haemoglobin concentration, colour index ratio were are carried out using Sigma Diagnostic kits [48].

On the 30th day after creating the wound, one animal from each group was anesthetized. Healed tissue along with normal skin at the two ends was excised for measuring tensile strength (MPa) and percentage of elongation at break (%) using a Universal testing machine (Instron model 4501). The break load was measured and the tensile strength was calculated using the following equation:

Tensile strength = Break load / strip cross sectional area

Statistical analysis

The results were expressed as mean±standard deviation (SD) of three individual experiments (n=3). The statistical analysis was performed using t-test. The significant difference level is $p \leq 0.05$.

Acknowledgments

R. Deepachitra gratefully acknowledges the financial support provided by Department of Science andTechnology (DST)

References

[1] S. Park, R. S. Rodney,*Nat. Nanotechnol.*, 2009, **4**, 217–224.

[2] O.C. Compton, S. T. Nguyen,*Small*, 2010, **6**, 711–723.

[3] A.K. Geim, K.S. Novoselov,*Nat. Mater.*, 2007, **6**, 183–191.

[4] C. Chung, Y.K. Kim, D. Shin, S.R. Ryoo, B. H. Hong, D.H. Min, *Acc.Chem.Res,* 2013, **46**, 2211-2224.

[5] S. Goenka, V. sant, S. Sant, *J Control Release,* 2014, **173**, 75-88.

[6] Y. Yang, A. M. Asiri, Z. Tang, D. Du, Y. Lin, *Materials today,* 2013, **16**, 365-373.

[7] K. Yang, J. Wan, S. Zhang, Y. Zhang, S. T. Lee, Z. Liu, *ACS Nano,* 2011, **5**, 516–522.

[8] W. Hu, C. Peng, L.V. Min, X. Li, Y. Zhang, N. Chen, C. Fen, Q. Huang, *ACS Nano,*2011, **5**, 3693–3700.

[9] O.N. Ruiz, K.A. Fernando, B. Wang, N.A. Brown, P.G. Luo, N.D. McNamara, M. Vangsness, *ACS Nano*, 2011, **5**, 8100–8107.

[10]K.Turcheniuk, M. Khanal, A. Motorina, P. Subramanian, A. Barras, V. Zaitsev, V. Kuncser, A. Lec, A. Martoriati, K. Cailliau, J.F. Bodart, R. Boukherroub, S. Szunerits, *RSC Adv* 2014, **4**, 865-875.

[11] G. Gollavelli G, Y.C. Ling, *Biomaterials*,2012, **33**, 2532–2545.

[12] Z. Sun, P. Huang, G. Tong, J. Lin, A. Jin, P. Rong, L. Zhu, L. Nei, G. Niu, F. Cao, X. Chen, *Nanoscale*, 2013, **5**, 6857-6866.

[13] B. Lu, T. Li, H. Zhao, X. Li, C. Gao, S. Zhang, E. Xie, *Nanoscale*, 2012,**4**, 2978-2982.

[14] S. Swarnalatha, A. Ganesh Kumar, S. Tandaiah, G. Sekaran, *J Chem Technol Biotechnol*, 2009, **84**, 751–760.

[15] L.F. Cabeza, M.M. Taylor, G.L. DiMaio, E.M. Brown, W.N. Marmer, R. Carrio, P.J. Celma, J. Cot, *Waste Manage*., 1998, **18**, 211–218.

[16] G. Bilgen, G. Oktay, Z. Tokgoz, G. Guner, S. Yalcin,*J. Vet. Anim. Sci.,* 1999, **23**, 483-487.

[17] T. Nagai, M. Izumi, M. Ishii, *Int.J. Food Sci. Technol*., 2004, **39**, 239-244.

[18] M. Sadowska, I. Kolodziejska, C. Niecikowska. *Food Chem*., 2003, **81**, 257-262.

[19] M.J. Fonseca, M.A. Alsina, F. Reig, *Biochim Biophys Acta*., 1996, **1279**, 259–265.

[20] M. Maeda, S. Tani, A. Sano, K. Fujioka, *J Control Release*, 1999, **62**, 313–324.

[21] W. Bensaid, J.T. Triffitt, C. Blanchat, K. Oudina, L. Sedel, H. Petite, *Biomaterials* 2003, **24**, 2497–2502.

[22] Q. Ye, G. Zund, P. Benedikt, S. Jockenhoevel, S. P. Hoerstrup, S. Sakyama, J.A. Hubbell, M. Turina, *Eur J CardiothoracSurg,* 2000, **17**, 587–591.

[23] S.L. Rowe, S. Lee, J.P. Stegemann.*ActaBiomater,* 2007, **3**, 59–67.

[24] S.E. Noorjahan, T.P. Sastry. *J Biomed Mater Res B ApplBiomater*., 2004, **71**, 305-312.

[25] J.S. Boateng, K.H. Matthews, H.N Stevens , G.M. Eccleston. *J Pharm Sci.,* 2008, **97**, 2892-2923.

[26] S.E. Noorjahan, T.P. Sastry, *J. Polym. Sci. A: Polym. Chem*., 2004, **42**, 2241-2252.

[27] J. Sathian, T.P. Sastry, L. Suguna , Y. Lakshminarayana, G. Radhakrishnan, *J Biomed Mater Res A*., 2003, **65**, 435-440.

[28] T.P. Sastry, C. Rose, S. Gomathinayagam, G. Radhakrishnan, *J. Appl. Polym. Sci.*,1998,**68**, 1109–1115.

[29]N. Natarajan, V. Shashirekha, S.E. Noorjahan, M. Rameshkumar, C. Rose, T.P. Sastry, *J MacromolSci A.,*2005, **42**, 945–953

[30] R.Y.N. Gengler, A. Veligura, A. Enotiadis, E.K. Diamanti, D. Gournis, C. Jozsa, B.J. Van Wees, P. Rudolf,*Small*, 2009, **6**, 35-39.

[31]J.M. Pachence, R.A. Berg, F.H. Silver, *Med. Device DiagnInd*., 1987, **9**, 49–55.

[32] K. Wang, J. Ruan, H. Song, J. Zhang, Y. Wo, S. Guo, D. Cui, *Nanoscale Res. Lett*., 2011, **6**, 1-8.

[33] J. Kim, L.J. Cote, F. Kim, W. Yuan, K.R. Shull, J. Huang,*J. Am. Chem. Soc*., 2010, **132**, 8180–8186.

[34]D. Lichtenberg D, E. Opatowski E, M.M. Kozlov, *Biochim. Biophys.Acta*, 2000, **1508**, 1–19.

[35]N. Muruthy, I. Chang, P. Stayton, A. Hoffman, *MacromolSymp*., 2001, **172**, 49–55.

[36]K. Yang, J. Wan, S. Zhang, B. Tian, Y. Zhang, Z. Liu,*Biomaterials*, 2012, **33**, 2206-2214.

[37]A. Thubagere, B.M. Reinhard,*ACS Nano* 2010, **4**, 3611-3622.

[38] J.R. Gurr, A.S.S. Wang, C.H. Chen, K.Y. Jan, *Toxicology*, 2005, **213**, 66-73.

[39]C. Peng C, W. Hu W, Y. Zhou Y, C. Fan, Q. Huang, *Small*, 2010, **6**, 1686-1692.

[40] N. Bryan, H. Ahswin, N. Smart, Y. Bayon, S. Wohler, J.A. Hunt, *Eur. Cell. Mater.,* 2012, **24**, 249-265.

[41] J.S. Boateng, K.H. Mathews, H.N.E. Stevens, G.M. Eccleston, *J. Pharm. Sci.,* 2008, **97**, 2892-2923.

[42]C.C. Wang, C.H. Su, C.C. Chen, *J. Biomed.Mater.Res .,* 2008, **84**, 1006-1017.

[43]J. Adam, M.D. Singer, A.F. Richard, M.D. Clark. *N Engl J Med.,* 1999, **341**, 738-746

[44]S. Enoch, D.J. Leaper, *Surgery*, 2008, **26**, 31-37.

[45]M.L. Noorlander, P. Meli, A. Jonker, C.J.F. Van Noordeen. *J Histochem Cytochem* 2002, **50**, 1469-1474.

[46] J.M. Trownbridge, R.L. Gallo, *Glycobiology*, 2002, **12**, 117-125

[47] V. Ramnath, S. Sekar, S. Sankar, C. Sankaranarayanan, T.P. Sastry, *J Mater Sci: MaterMed*., 2012, **23**, 3083–3095.

[48] S.A. Bidgoli, M. Mahdavi, S.M. Rezayat, M. Korani, A. Amani, P. Ziarati, *Acta Medica Iranica,* 2013, **51**, 203-208.

[49] W.S. Hummers, R.E. Offeman, *J Am Chem Soc.,* 1958, **80**, 1339–1339.

[50] T.P. Sastry, K.P. Rao, *J. of Bioact and Compat*.,1990, **5**, 430–438.

[51] T. Mosmann, *J. Immunol. Methods*., 1983, **65**, 55–63.

[52] P. Venkatesan, N. Puvvada, R. Dash, B.N. Prashanth Kumar, D. Sarkar, B. Azab, A. Pathak, S.C. Kundu, P.B. Fisher, M. Mandal, *Biomaterials*, 2011, **32**, 3794–3806.

[53] P. Khullar, V. Singh, A. Mahal, P.N. Dave, S. Thakur, G. Kaur, J. Singh, S.S. Kamboj, M.S. Bakshi, *J. Phys. Chem.,* 2012, **116**, 8834–8843.

[54] T. Wang, L. Qin, B. Liu, Y. Liu, B. Wilson, T.E. Eling, R. Langenbach, S. Taniur, J.S. Hong, *J. Neurochem*., 2004, **88**, 939-947.

[55] J.F. Woessner. *Biochem J*., 1962, **83**, 304-314.

[56] L.A. Elson, W.T.J. Morgan. *Biochem J*. 1933, **27**, 1824–1828.

[57] P.W. Morgen, A.G. Binnington, C.W. Miller, D.A. Smith, A. Valliant, J.F. Prescott. *Vet Surg*. 1994, **23**, 494–502.

[58] S. Schiller, A.G. Slover, A. Dorfman A. *J Biol Chem*., 1961; **236**, 983–987.

[59] T. Bitter, H.M. Muir, *Anal Biochem*., 1962, **4**, 330-334.